Density-functional study of Sc_n ($n=2-16$) clusters: Lowest-energy structures, electronic structure, and magnetism

H. K. Yuan,[1,2] H. Chen,[1,*] A. S. Ahmed,[1] and J. F. Zhang[1]
[1]*School of Physical Science and Technology, Southwest University, Chongqing, 400715, People's Republic of China*
[2]*School of Physical Science and Technology, Suzhou University, Suzhou, 215006, People's Republic of China*
(Received 31 March 2006; revised manuscript received 12 June 2006; published 31 October 2006)

The all-electron spin-polarized generalized gradient approximation (GGA) to the density-functional theory (DFT) has been used to determine the binding energies, ground-state structures, electronic structures, and magnetic properties of Sc_n clusters ($n \leqslant 16$). The ground-state structures are closed compact arrangements and the clusters containing 4, 5, 7, 10, and 13 atoms are found to be more stable than their neighboring clusters. The results for the net magnetic moments and their evolution with size for the optimal clusters are in good agreement with experiment. Clusters favor lower spin configurations except for Sc_2, Sc_{13}, and Sc_{14} clusters. Sc_{13} cluster is a perfect icosahedral structure with a giant magnetic moment of $19\mu_B$ and the maximum peak at Sc_{13} in experiment is reproduced by our calculations. Although our calculations overestimate some of the values, the size-dependent trend is generally consistent with the experimental pattern. The origin of the discrepancies arising in some cases is also discussed.

DOI: 10.1103/PhysRevB.74.144434 PACS number(s): 75.50.Xx, 36.40.Cg, 73.22.−f

I. INTRODUCTION

According to Hund's rules, magnetism exists in isolated atoms of 3*d*, 4*d*, and 5*d* transition-metal (TM) elements because all of them have unfilled localized *d* states. However, only a few 3*d* (Fe, Co, Ni) are found to form ferromagnetic materials in solids. Since a cluster is an object that lies between an atom and bulk, it is accepted that TM clusters containing fewer than 100 atoms can exhibit magnetic ordering not displayed by the corresponding bulk solids.[1–4] The development in experimental methods over the past few years has enabled scientists to generate, characterize, and study clusters of any size and composition. When combined with the experimental approach, the first principles method based on density functional theory[5,6] (DFT) is proved to be effective in cluster research, especially in predicting the geometrical structure.

The most important characteristics intrinsically related to magnetic properties[4] are the lowest energy geometrical structure and respective electronic properties, which can determine the ground state and excited state properties. These two sides are not independent, although it is a common approximation to separate them due to the computational costs involved in fully self-consistent calculations. A structural optimization, as we know, changes both the bondlengths and point-group symmetry of a cluster. The former addresses the change on bonding due to an uniform expansion or compression of the cluster, thus providing information on the electronic localization-delocalization mechanisms that are know to be fundamental in TM clusters, the latter is mainly concerned with the change in magnetism to different symmetry.[7] Therefore, for any given cluster size, theoretical calculations generally reveal several nearly isoenergetic isomers, making definitive identification of the actual ground state structures difficult. From experimental side, it is possible that multiple isomers are also produced in experiment, in which case the elucidation of structures by comparing experiment and theory is much less straightforward. However, because the isomers often display widely varying magnetic moments, the experimentally determined values can be used to identify the isomer actually produced in the experiment or at least to rule out unlikely candidates.[2]

For clusters of 3*d* series, the Fe, Co, Ni ferromagnetic element clusters have been comprehensively studied, and both theories and experiments shown that they have enhanced magnetic moments in clusters. However, for other nonferromagnetic 3*d* TMs such as V and Cr, theoretical calculations[8] predicted large magnetic moments in both clusters, whereas, experimental measurements[9] have given almost nonmagnetic results. As with most transition elements, scandium is paramagnetic in its bulk phase, but the relatively high paramagnetic susceptibilities,[10] as compared to those of its neighbors in the Periodic Table, suggest that it is on the verge of ferromagnetic instability, and may be induced to display magnetic ordering by spatial confinement. Furthermore, Sc atom in its ground state electronic configuration ($[Ar]\ 3d^1 4s^2 4f^0$) possesses a single 3*d* electron, so a relatively simple but interesting case is the growth behavior of scandium clusters. The odd number of valence electrons in the scandium atom as well as the narrowing band could cause the enhancement of magnetism in small clusters. Finally, for small scandium clusters there are currently no theoretical studies on the structural growth behavior and the magnetic properties to provide guidance as to the nature of their magnetic ordering. The only available information are a few experimental[11–13] and quantum chemical calculational results[14,15] on dimer of Sc_2 with empirical method. More recently, small scandium clusters (Sc_2-Sc_{20}) were subject to investigations of the dependence of magnetic moments on cluster size using a Stern-Gerlach molecular-beam deflection experiment.[13] The results suggested that the scandium clusters exit in the lower spin states except for Sc_{13} cluster, which shows the highest magnetic moments of $6.2\mu_B$ that is different from those obtained for others. Note that the size dependencies of the total moments in experiment do follow a simple odd-even pattern approximately (e.g., between 1 and

$2\mu_B$) for most Sc_n clusters indicative of alternating doublet and triplet spin states, as was recently reported for niobium clusters.[16] The experimental observations have stimulated us to identify the lowest energy geometrical structures and determine the respective magnetic properties.

We have performed a comprehensive density function theory study on Sc_n clusters ($n=2-16$), with the aim to explore the geometrical structure growth and the evolution of the magnetic properties in the light of the experimental results. A lot of compact geometries have been considered for finding the equilibrium structures, and possible electronic configurations of total spins for several most favorable structures were tried to confirm the ground state. The exceptional stabilities of 13-atom clusters (Sc_{13}, Y_{13}, and La_{13}) have been further explored in order to find the commonality of the electronic structure and the magic behavior. In what follows, we will first describe computational methodology used in the work, including a technique for efficiently scanning the energy surface for favorable structures in Sec. II, and then present our results and discussion in Sec. III. Finally, a summary is given in Sec. IV.

II. COMPUTATIONAL PROCEDURE

All calculations were performed using the density functional theory (DFT) provided by the DMOl3 package.[17] The density functional is treated with general gradient approximation (GGA) corrected-exchange potential of BPW [constructed by combining the Perdew and Wang (PW) correlation functional with Becke's exchange functional].[18,19] We have chosen a basis set composed of double numerical basis ($3d$ and $4s$) with polarized function ($4p$) (DNP), and all-electron spin-unrestricted calculations are performed. For accurate evaluation of the charge density, we have chosen the octuple scheme for the multipolar fitting procedure and a fine grid scheme for numerical integration. The convergence criterion of optimization is set to 1×10^{-5} eV/Å for the energy gradient and 5×10^{-4} Å for the atomic displacement. The charge density is converged to 1×10^{-6}, which allow a total energy convergence of 1×10^{-5} eV.

The ground state structures of Sc_n ($n=2-16$) and preferred spin multiplicities are obtained from the maximum in the binding energy (E_b). The E_b of a cluster is defined as $E_b=E_t-E_a$, where E_t is the sum of each atomic energy and E_a is the total energy of the cluster. Usually, a single determinant scheme is a highly inadequate approximation to a magnetic system with sizeable spin. In most cases this approach led to the lowest spin isomer, whereas, in some case the energy differences between the different spin isomers are quite small especially for larger clusters due to their very smooth potential surface, and we might not obtain the actual ground state. Therefore, to determine the ground states of Sc_2-Sc_{16} clusters efficiently, we divided the optimization procedure into two steps. In the first step, we calculated the ground state energy for a large number of geometries for the Sc_n clusters of each size. As the cluster size increases, the number of possible geometries increases dramatically. The energy surface of even a seven-atom scandium cluster is complicated and the unbiased searches of the configuration and spin multiplicities at first-principles level are computationally very demanding. So, as initial geometries we started with the structures of analogous sizes that have been discussed previously.[16,20–25] In addition, we tried a large number of different geometries that were derived from previously calculated structures. For example, for many clusters one can describe the geometry as a superposition of smaller building blocks that typically are trigonal, tetragonal, pentagonal, or hexagonal pyramid geometries. Thus, we can often simply add or subtract an atom from a cluster of size n to obtain geometry for a cluster of size $n+1$ or $n-1$. In this manner, we typically generated from 10 to 30 different geometries or the geometries with different symmetries for each size. In all, more than 300 configurations were relaxed to ensure thorough exploration of the potential energy surfaces of the clusters. However, it is possible that for certain cluster sizes (in particular, the larger ones) we did not find the correct ground state structures. Initial structures were first set in the highest possible symmetries. A full geometry optimization was then carried out without any symmetry constraint. If the initial symmetry did not change after the calculation, a low symmetric input was also tested to ensure that the result is not affected by initial symmetric input and that one may not end up with a local minimum. The optimal spin configurations are determined automatically as the calculation is done at each self-consistent iteration. It is also found that the occurrences of degenerate states promote distortions from the most compact or high symmetric geometries. In fact, slightly distorted structures are often more favorable than highly symmetric ones.

In the second step, for several energetically most favorable structures of each cluster size, which are detected in the first step, we fully reoptimized possible electronic configurations of total spins without symmetry constraint. This gives a considerable number of states needed for the characterization of the potential energy surface: ground state and excited states for a given cluster. If such calculations are performed for several different fixed moments, a binding energy curve is obtained from which all possible metastable states could be determined. In this procedure, the system is forced to have a fixed magnetic moment, defying the ordinary Fermi occupation rule. In view of the cluster sizes involved in this project, consistent use of the appropriate multiconfiguration approach is not possible.

We have found that the abovementioned simple procedure allows a systematic and accurate study of these complex systems. The calculations of the equilibrium geometry, electronic structure, magnetic moment, and binding energy were carried out for Sc_n clusters for $n=2-16$, using the data from the most stable structure when more than one isomers are available. Mulliken population analyses were done to obtain both the charges on each atom and unpaired spin populations. The accuracy of the current computational scheme has been checked by benchmark calculations on the scandium dimer. For the Sc_2 dimer, the E_b and bondlength are obtained as 1.978 eV and 2.647 Å, which compare well with other theoretical work.[14,15] Up to now, no experimental data are available for the equilibrium bondlength and E_b of the scandium dimer. Our calculated spin multiplicity and vibration frequency of Sc_2 (5 and 263.7 cm^{-1}, respectively) are in

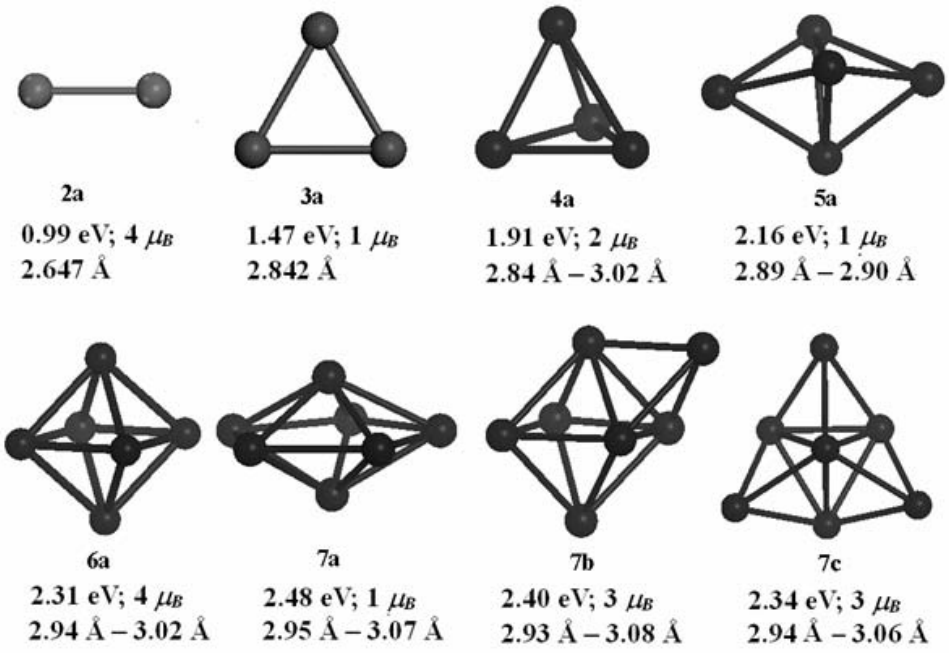

FIG. 1. Some of the isomers found for Sc_n clusters ($2 \leqslant n \leqslant 7$), with their binding energies/atom, total magnetic moments, and nearest-neighbor distances. Isomer *na*, *nb*, or *nc* are the *m*th least energetic isomers with *n* atoms (among isomers with the same configuration, only that with the greatest binding energy is counted).

agreement with the theoretical values given by Gutsev *et al.*[15] and compare favorably with the experimental value.[11,12]

III. RESULTS AND DISCUSSION

A. Equilibrium geometries of Sc_n ($n \leqslant 16$) clusters

Figures 1–3 show the structures, binding energies/atom (E_b/atom), total magnetic moments (in units of the Bohr magneton μ_B), and nearest-neighbor distances (NNDs) of some of the lowest-energy isomers found in our calculations for Sc_n clusters with n=2–7, n=8–11, and n=12–16, respectively (when the same geometry is shared by more than one isomer with different NNDs, only the most stable isomer is shown). The isomers are labeled with two indices: the first (number) represents the number of atoms in cluster and the second (letter) ranks the isomers in decreasing order of binding energy.

For Sc_3, we examined three possible geometries of equilateral, isosceles, and arbitrary triangles with D_{3h}, C_{2v}, and C_s symmetries. The ground state is an equilateral triangle (D_{3h}) with a bondlength of 2.84 Å and a binding energy of 1.47 eV/atom, which is more stable than the isosceles and arbitrary triangles by 0.03 and 0.11 eV/atom, respectively. It is a spin doublet state. Sc_4 is the smallest cluster that could display a three-dimensional structure. Consequently, we optimized the geometries subject to three-dimensional T_d, D_{2d}, C_{3v}, C_s as well as planar D_{2h}, C_{2h}, and C_{2v} symmetries. The ground state is a distorted tetrahedron (D_{2d}) with an average bondlength of 2.90 Å and a binding energy of 1.91 eV/atom. It is a spin triplet state. The tetrahedron (T_d) and other distorted tetrahedrons (C_{3v} and C_s) are 0.03, 0.05, and 0.01 eV/atom above the ground state. For Sc_5, we considered the square pyramid with C_{4v}, C_{2v} symmetries and the triangular bipyramid with D_{3h}, C_{3v}, C_{2v}, and C_s symmetries. The ground state corresponds to the triangular bipyramid (D_{3h}) with average bondlength of 2.90 Å and a binding energy of 2.16 eV/atom, which is more stable than the triangular bipyramid (C_{2v}) and the square pyramid by 0.05 and 0.11 eV/atom, respectively. It is a spin doublet state. The spin quartet and sextet states with the same geometry are 0.05 and 0.01 eV/atom above the ground state, respectively.

For Sc_6, we examined the tetragonal bipyramid with O_h, D_{3d}, D_{4h}, D_{2h} symmetries and the pentagonal pyramid with C_{5v} symmetry. Furthermore, the capped trigonal bipyramid with C_{2v} symmetry and the prism with D_{3h} symmetry are also considered. The ground state structure (D_{4h}) with an average bondlength of 2.97 Å and a binding energy of 2.31 eV/atom, which is 0.02 eV/atom lower than the O_h octahedron, can be regarded as the outcome of a small Jahn-Teller distortion from the O_h structure. It is a quintet state. The triplet and septet states are 0.03 eV/atom above the ground state. The D_{5h} pentagonal bipyramid (PBP) (7*a*) with a spin doublet state is the lowest energy configuration for Sc_7. It has a binding energy of 2.48 eV/atom and average bondlength of 2.99 Å. In addition, capped octahedron (7*b*), tricapped tetrahedron (7*c*), and bicapped square pyramid are considered. However, these isomers are higher in energy than ground state. For Sc_8, a tetragonal antiprism relaxes to an adjacent bicapped octahedron with C_{2v} symmetry (8*a*) and lies 0.04 eV/atom below a capped PBP (8*b*). Both structures are triplet states. The third lowest energy isomer of Sc_8 is an opposite bicapped octahedron with D_{3d} symmetry (8*c*) which is 0.06 eV/atom higher than ground state (8*a*). For Sc_9, the ground state structure, which is a doublet state, is a bicap-

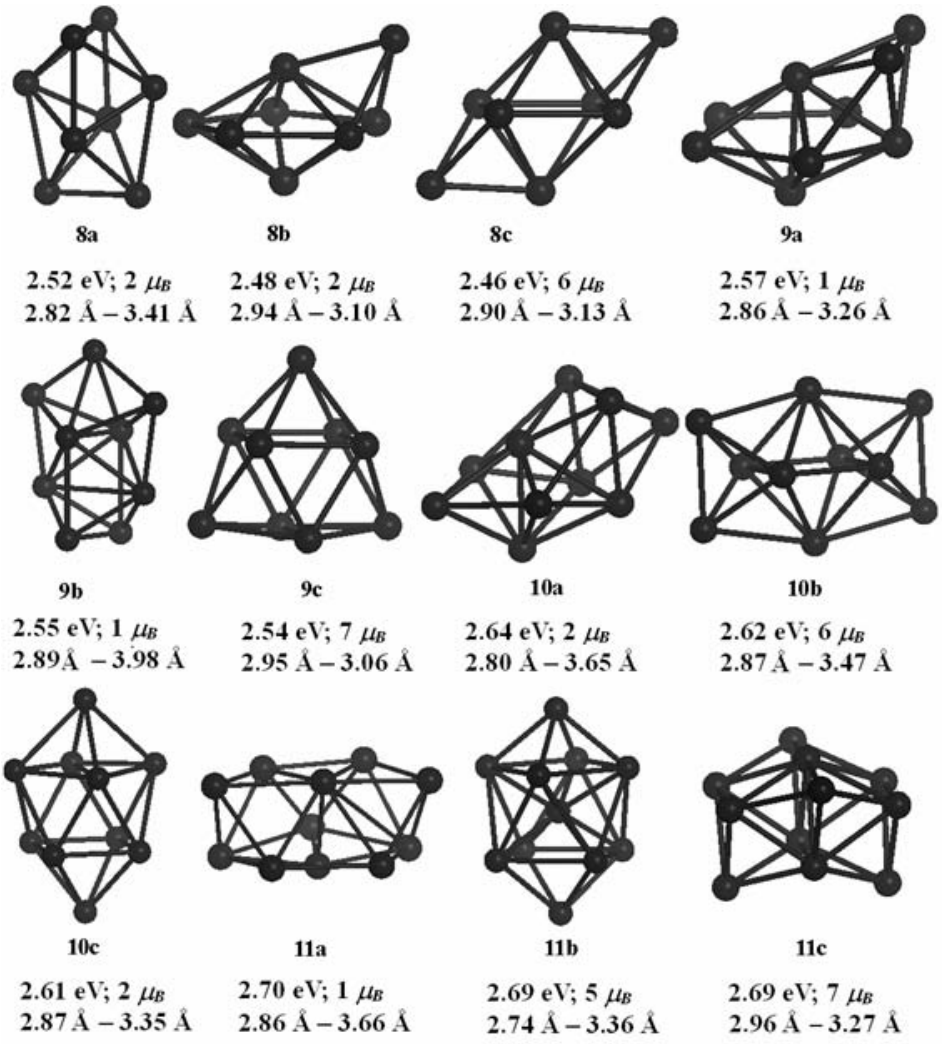

FIG. 2. As for Fig. 1, but for $8 \leqslant n \leqslant 11$.

ping of adjacent faces on the same side of a PBP with C_s symmetry (9*a*). The D_{3h} tricapped prism (9*c*) lies 0.03 eV/atom higher in energy than isomer (9*a*). Another isomer (9*b*) with capping of two adjacent faces on opposite sides of the basal plane of a PBP is 0.02 eV/atom higher than ground structure (9*a*).

For Sc_{10}, three lowest energy isomers are obtained: tricapping of adjacent faces on the same side of a PBP with C_s symmetry (10*a*), quartetcapped octahedron (10*b*), and bicapped tetragonal antiprism (10*c*). The ground state corresponds to an isomer (10*a*) with a binding energy of 2.64 eV/atom. It has a spin multiplicity of 3. Three lowest energy isomers for Sc_{11} cluster are shown in Fig. 2 (11*a*, 11*b*, and 11*c*). The ground structure with a binding energy of 2.70 eV/atom (11*a*) can be described as a layered structure (one layer has six atoms and another has five atoms). It is a spin doublet state. The other two isomers can be obtained by embedding one atom in a bicapped tetragonal antiprism (11*b*) or by fusing two octahedrons at a triangular face then adding two atoms on each side of the axis (11*c*). The lower-lying isomers of Sc_{12}-Sc_{16} clusters are shown in Fig. 3. The results predicate that the lowest structures of Sc_{12}, Sc_{13}, and Sc_{16} clusters are isomers based on icosahedral packing (see Fig. 3). The ground state structure of Sc_{12} can be described as a distorted bicapped pentagonal antiprism with C_s symmetry (12*a*). It is only 0.01 eV/atom lower in energy than next two isomers (12*b* and 12*c*). With such small energy difference, these isomers are likely to be present in experiments. For Sc_{13}, it has a perfect I_h icosahedral configuration with bondlengths in the range 3.02–3.16 Å. The distorted icosahedrons with lower symmetries (D_{5d}, D_{3d}, and D_{2h}) are found to be much higher in energy than I_h structure. In addition, truncated decahedral (D_{5h}), bcc (D_{4h}), hcp (D_{3h}), and cuboctahedral (fcc O_h) are calculated. Similar geometries are often considered in other transition metal clusters from previous theory calculations.[24–28] Finally, four lowest energy isomers of Sc_{13} (13*a*, 13*b*, 13*c*, and 13*d*) are obtained.

For Sc_{14}, we identified a capped icosahedron, a hexagonal layered structure, a fcc structure, and the structures of symmetric capping of the Sc_{13}. The lowest energy structure (14*a*) can be obtained by capping one atom on the icosahedral to form the C_{2v} symmetry. The next lower isomer (14*b*), which is only 0.02 eV/atom higher than the ground state structure (14*a*), is a capping of icosahedron on a threefold site with

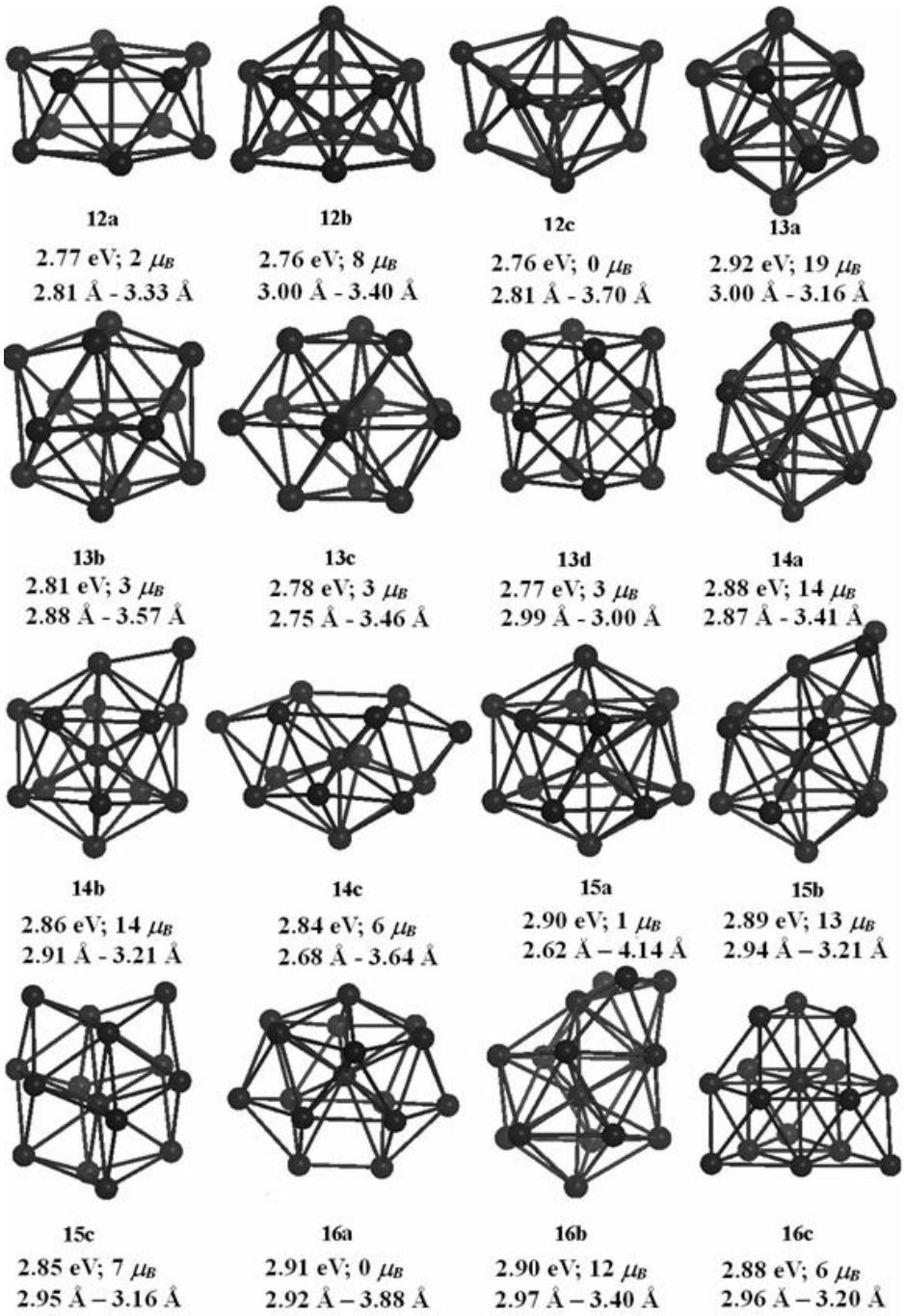

FIG. 3. As for Fig. 1, but for $12 \leqslant n \leqslant 16$.

C_{3v} symmetry. Note that the energy difference is very small. The results again indicate the existence of isomers with nearly degenerate energies. The most stable structure of Sc_{15} is a little distorted bicapped hexagonal antiprism with C_{3v} symmetry (15*a*). The next two stable isomers were found to be a bicapping on adjacent faces on icosahedron (15*b*) and a bicapping on hcp structure (15*c*). Lastly, our calculations predict that the ground structure of Sc_{16} (16*a*) would follow a growing pattern based on the geometry of Sc_{15} (see Fig. 3). It is a spin singlet state. The tricapped icosahedron structure (16*b*) is only 0.01 eV/atom higher than the isomer (16*a*). According to the above-noted analysis, one observed that all Sc_n ($n>3$) clusters are closed compact arrangements. It is notable that the differences of binding energies between the isomers for each size ($n>8$) are about 0.01–0.04 eV/atom which is less than 2% of the binding energy/atom of their systems. Given the error of approximation of exchange-correlation energy, we cannot determinately regard those isomers, which are slightly higher in energy than the corresponding ground state structure, as unstable.

B. Evolution of the structural and electronic properties

After affirming the lowest structure of the Sc_n ($n \leqslant 16$) clusters, we begin to discuss the evolutions of the inter-

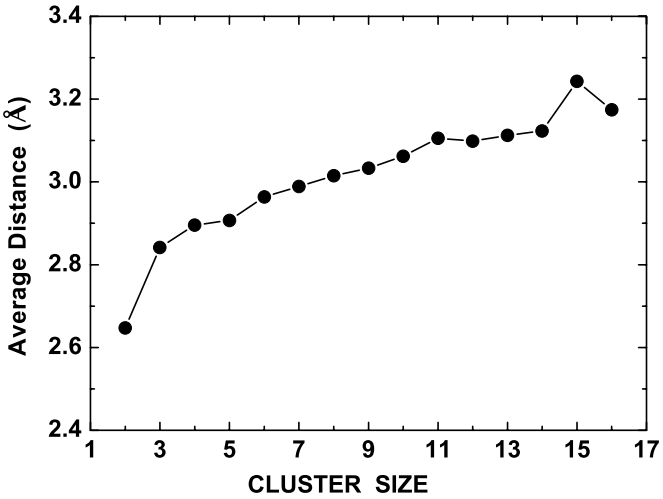

FIG. 4. Average interatomic distance as a function of cluster size.

atomic distance, binding energy/atom, highest occupied molecular orbital (HOMO) lowest unoccupied molecular orbital (LUMO) gap, ionization potential, electron affinity, and second difference of energies of Sc_n ($n \leqslant 16$) clusters.

As shown in Figs. 1–3, the interatomic distances vary between nearest-neighbor atoms in each of these clusters, we define the average nearest-neighbor distance $\bar{R}=(1/n)\Sigma_i R_i$, where i refers to the number of bonds in the cluster having a length of R_i. In Fig. 4, we plot $\bar{R}$ as a function of cluster size n. Note that it increases monotonically with cluster size except for a large jumping at Sc_{15}. The average nearest-neighbor distance of Sc_{15} is comparable to the bulk nearest-neighbor distance of 3.25 Å.[29] In Fig. 5, one plots the curve of binding energy/atom. It increases monotonically with size although the rate of increase decreases with size, and the curve does not exhibit strong quantum size effects or large jumps. The smooth variation seen in Fig. 5 suggests that even if more stable arrangements exist, their binding energies are unlikely to be significantly higher than those found here. The stability of Sc clusters can be qualitative explained

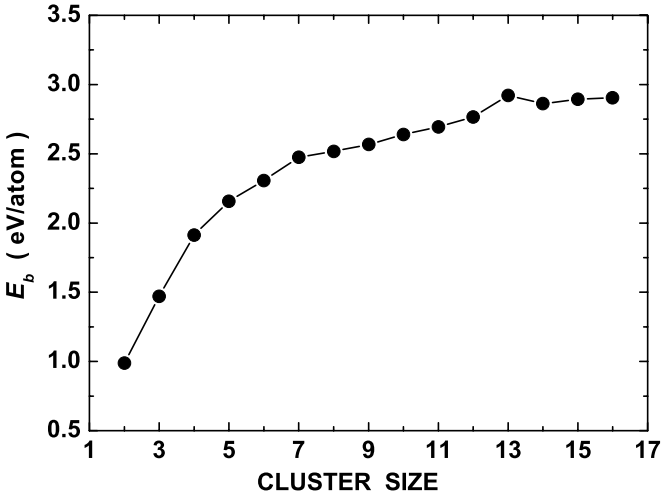

FIG. 5. Plot of E_b vs cluster size.

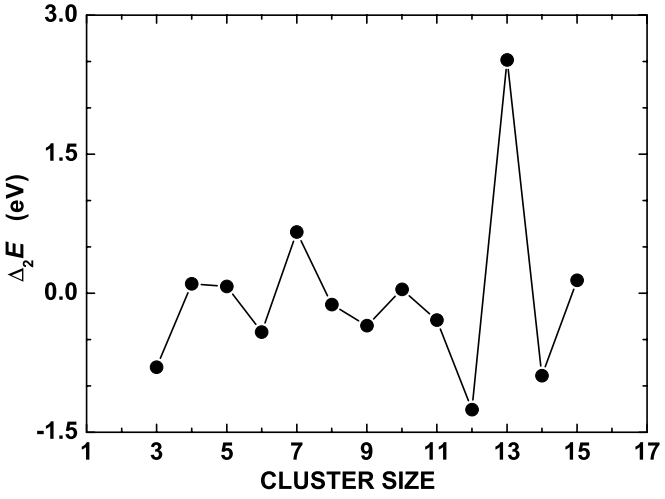

FIG. 6. Second differences of cluster energies.

by considering the chemical bonding and the magnetic interaction. On the one hand, a cluster usually tends to make the structure stable and compact by increasing the coordination and decreasing the interatomic distance to enhance its E_b, which would reduce magnetic moments because both factors tend to increase $3d$ electron delocalization. On the other hand, to increase the exchange splittings of d orbitals by reducing the strength of some bonds also can enhance the E_b, which would increase magnetic moments. As results of the competition, a cluster finally reaches its stable structure and magnetic state. From Fig. 5, it is difficult to predict the Sc clusters which are more stable than others as has been clearly demonstrated for simple metal clusters such as the alkali series. Thus, to study if any of these Sc clusters could be magic, we will investigate the second differences of total energies.

Figure 6 shows the second differences of total energies $\Delta_2 E(n)=E(n+1)+E(n-1)-2E(n)$, as a function of the cluster size n. The behavior of the variations is different to those of alkali and noble clusters which exhibit characteristic shell oscillations with respect to the cluster size. Peaks are found at $n=4$, 5, 7, 10, 13 implying that these clusters are more stable than their neighboring clusters. This trend is the same as the one observed in other transition metal clusters where seven-atom, ten-atom, and thirteen-atom clusters are often found to be magic.[23,30,31] The stable behaviors of $n=5$, 7, and 13 are in contrast to the sp bonded metal clusters for which the magic clusters have a very large HOMO-LUMO gap and in general clusters with odd number of electrons are not magic. Obviously, those stable clusters origin mainly from the compact atomic arrangements, and this definition can be illustrated by the Sc_{13} cluster easily. For the Sc_{13} cluster, the icosahedron is well established and frequently has been observed as a geometric magic number (13, 55, 147,…), furthermore, it holds 39 cluster valence electrons and still absents one electron to form the electronic magic numbers (8, 20, 40,…). Therefore, it suggests an important role of the geometrical compact arrangements of their stabilities. In addition, the Sc_{13} cluster possesses a HOMO-LUMO gap of 0.5 eV which is larger than its neighboring clusters (Fig. 7). Thus, large gaps and high ionization potential due to elec-

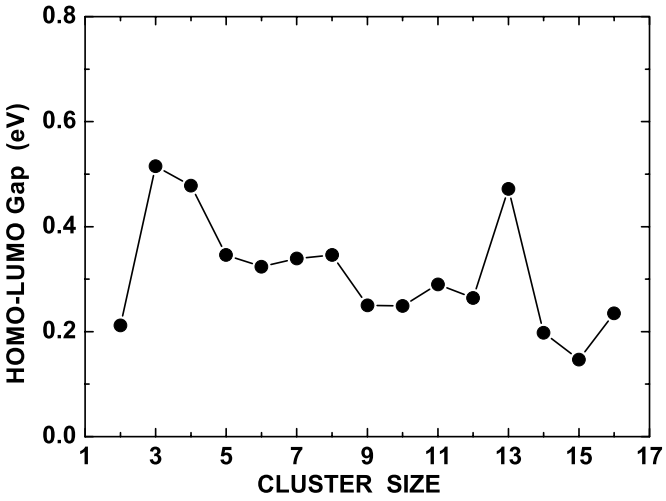

FIG. 7. HOMO-LUMO gap vs cluster size.

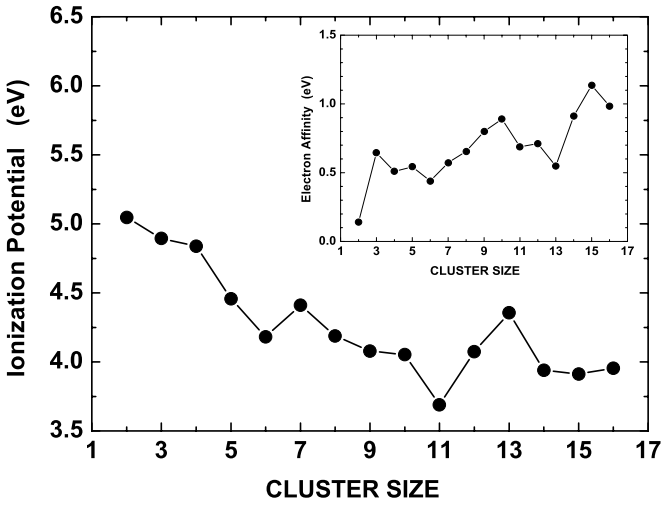

FIG. 8. Vertical ionization potentials and vertical electron affinity (inset chart) of Sc_n.

tronic shell closing also contribute to the stability to some extent. To our knowledge, there is no abundance spectrum of Sc clusters.

In order to reconfirm the most stable clusters as mentioned above, we now discuss the electronic properties of scandium clusters by examining the energy gap between the HOMO and LUMO. Large gaps are good indicators of the stability of clusters. In Fig. 7, one can see that all clusters have large gaps comparing with other transition metal clusters.[21,32] Most importantly, one finds that the clusters with n=3, 4, and 13 have lager gaps than other sizes. According to the Jahn-Teller theorem, nonlinear electronic system, which has orbital electronic degeneracy and high symmetry, is unstable,[33] especially in the systems whose HOMO is partially occupied. In our calculations, the possible Jahn-Teller distortions were investigated to obtain the most stable clusters. For example, if the structures obtained were open-shell electronic configurations, the structures would tend to distort further so as to lift the degeneracy of the ground states and higher their energies with a closed shell.

The ionization potential (IP) and the electron affinity (EA) have provided fundamental tools to insight into the size-dependent evolution of electronic structures and to distinguish isomers that possess different energies. The vertical IP is the difference between the binding energies for Sc_n^+ and Sc_n clusters at the geometry of the maximum binding energies for Sc_n clusters. The vertical EA is evaluated by adding one electron to the Sc_n cluster in its equilibrium geometry then taking the difference between their binding energies. We have calculated the IPs and the EAs of the Sc_n clusters, and plotted the results in Fig. 8. The higher IPs are found at n =2–4, furthermore, significant oscillations around the magic-sized clusters such as Sc_7, Sc_{13} are obtained. For other size, the IPs decrease gradually with cluster size. These phenomenon further verify that the Sc_4, Sc_7, Sc_{13} clusters are the most stable species. The low (high) EA of a cluster is identified as a signature of a closed-shell (open-shell) pattern of electronic configuration with large (small) HOMO-LUMO gap. Comparing the overall trends of the gaps and the EAs, we observed that there is an obvious contrast between their systematic trends. For example, the EAs of Sc_{10} and Sc_{15} clusters are situated on the peaks of the curve in the inset in Fig. 8, while the gaps of the corresponding clusters are at the depressed positions in the behavior in Fig. 7. There are currently no available experimental data on IPs and EAs of small Sc clusters.

C. Magnetic moments of Sc_n clusters

As mentioned in the Introduction, the most interesting property of scandium clusters is that bulk Sc is paramagnetic, but the experiment shows that the magnetic moments in Sc clusters change nonmonotonically with cluster size. Thus, scandium clusters may serve as an ideal system to understand the interplay between size, geometry, electronic structure, and magnetism. Detailed data on the magnetic behavior of scandium clusters in the size range of 2–20 atoms have very recently become available from molecular beam deflection experiment.[13] In Fig. 9, our theoretical results (open circles) are compared well with the experimental val-

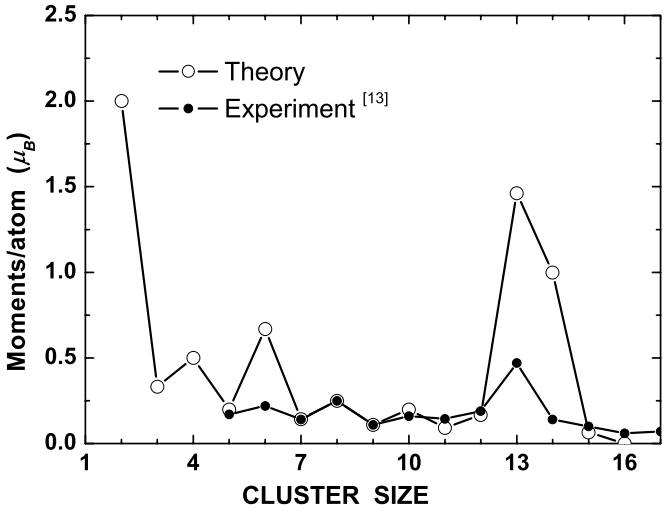

FIG. 9. Variation of magnetic moments (μ_B/atom) as a function of cluster size.

ues for Sc_n (n=5, 7–12, 15, and 16), however, there are significant differences for the clusters containing 6, 13, and 14 atoms. Although our calculations overestimate these three values, the size-dependent trend is generally consistent with the experimental trend. The even-odd alternation (the clusters have total magnetic moments $1\mu_B$ for n=3, 5, 7, 9, 11, 15 but $2\mu_B$ for n=4,8,10,12) in cluster magnetism may be due to the odd number of valence electrons in the Sc atom. The pronounced oscillations of the magnetic moment that give a strong increase for Sc_6 and Sc_{13} clusters were suggested to occur as a consequence of the symmetry in the geometrical structure. The maximal peak at Sc_{13}, which is considerably larger than the value of $6\pm0.2\mu_B$ measured in the experiment, is also reproduced in our calculations.

The experiment measured only the total magnetic moments of clusters and there is no direct indication of the nature of the magnetic ordering displayed by these cluster systems. In fact, the magnetic behavior can be ferromagnetic (FM), where spins are aligned in parallel directions, antiferromagnetic (AFM), where the spins are antiparallel, or noncollinear, where the spins are not parallel and may be disordered. Almost all theories to date employed the DFT with the assumption that spins are automatically collinear along a fixed quantization axis. In order to make clear the magnetic properties of Sc clusters, further investigations were required. Analyzing the atomic magnetic moments of every atom of the lowest Sc_n clusters (detailed data are not given), we found that the atomic magnetic moments are small but nonzero. Additionally, it is observed that the clusters undergo a change from ferromagnetic (FM) ordering for the smallest sizes ($n<7$) to antiferromagnetic (AF) ordering for the intermediate sizes (n=7–12,15–16). Notable exceptions are Sc_{13} and Sc_{14} clusters with per atom moments of $1.46\mu_B$ and $1\mu_B$, respectively, thus putting these clusters in the class of FM ordering. The superparamagnetic behavior of Sc clusters in the experiment[13] should be interpreted by spin arrangements. The atoms have small individual moments for Sc_2-Sc_7 clusters, which prefer FM ordering, but AF ordering is clearly favored for the intermediate sizes, in which the atomic moments remain slightly large but their orientations flip from site to site. Therefore, the net moments of these clusters are small. In addition, by examining the three lowest isomers for each cluster size, we find that for small clusters the most stable magnetic configurations of those isomers are FM ordering, while for larger clusters the isomers with FM ordering are close in energy to the ground-state structure with AF ordering. In all the cases, the magnetic ordering is closely related to geometry. The spatial symmetry and the local coordination number of each atom are changing and play a major role in the magnetism of the Sc cluster, and the exchange interaction between electrons determine the magnetic ordering. In view of the possibility of AF ordering in these clusters, the relative orientations of the individual atomic spins in lowest-lying isomers should be considered in the future optimization process.

Furthermore, Kohl and Bertsch[34] found that small Cr_n clusters ($n<13$) strongly favor noncollinear configurations of their local magnetic moments due to frustration. This effect is associated with a significantly lower total magnetization of the noncollinear ground states, making the disagreement between Stern-Gerlach measurements[9] ($\mu<0.77\mu_B$/atom) and previous collinear calculations for Cr_{12} ($1.67\mu_B$/atom) and Cr_{13} ($1.06\mu_B$/atom) clear.[35] Their results further suggest that the trend to noncollinear configuration might be a feature common to most antiferromagnetic clusters but would be less dramatic in other transition metals. These phenomena are also found in Mn clusters.[36,37] In light of the trend from Cr_{12} and Cr_{13} clusters, it is a reasonable hope that noncollinear effects might largely reduce the difference between the theory and experiment for Sc clusters, especially for Sc_{13} and Sc_{14} clusters.

In addition, unlike the situation in bulk transition metals, orbital contribution may be significant in small transition metal clusters. Recently, using a tight-binding scheme which includes spin-orbit interactions, Guirado-Lopez *et al.*[38] studied the orbital magnetic moments of the TM cluster and obtained $0.2-0.4\mu_B$/atom ($n\leqslant13$) for Ni clusters and $0.1-0.18\mu_B$/atom ($n\leqslant19$) for Rh clusters. The nonicosahedral structures of Rh_n as compared to Ni_n clusters tend to diminish the orbital moments. Then, with orbital correlation and spin-orbit interactions, Wan *et al.*[39] also confirm that the disagreement between experiments and theoretical works is due to the neglect of orbital contribution. It is found that in Ni clusters the effect of spin-orbit coupling on magnetic values is almost negligible. In our case, taking into account the largest enhanced orbital moments $0.4\mu_B$/atom as in Ni clusters, which in Sc clusters align antiparallel to the spin moments, we cannot remove the largest part of the discrepancy of magnetic magnitude for Sc_{13} and Sc_{14}. Furthermore, the larger atomic radii of Sc compared to other 3*d* TM would be related to weaker correlation effects, which should favor electron delocalization leading to less atomiclike orbital moments and possibly to a further decrease of orbital moments.

For Sc_{13} cluster, the discrepancy of magnetic moments between theory and experiment is so large that possible isomers and various spin multiplicities should be examined. First, we considered the icosahedrons with different symmetries and found that the binding energies of those lower-symmetry icosahedrons are lower than that of I_h icosahdedron (I_h: 37.99 eV and $19\mu_B$; D_{5d}: 35.88 eV and $9\mu_B$; D_{3d}: 36.08 eV and $15\mu_B$; D_{2h}: 36.04 eV and $13\mu_B$). Furthermore, as mentioned above, the truncated decahedral (D_{5h}), bcc (D_{4h}), hcp (D_{3h}), and cuboctahedral (O_h) structures were tried. After extensive calculations, four lower energy isomers of Sc_{13} were given in Fig. 3. The I_h icosahedron is the ground state structure with $=19\mu_B$, and other three isomers with $3\mu_B$ magnetic moments are about 0.11–0.15 eV/atom higher in energy than the ground state. Although latter three isomers are higher in energy, the predicted magnetic moments lie below the experimentally determined value. The small moments of these isomers can diminish the difference between experimental and theoretical values. From another side, with regard to the ground state structure obtained above, we should examine whether the excited states lie energetically close to the ground state. Figure 10 shows the binding energies for spin moments of those isomers. For most isomers, the binding energies change very little as the moments change from $1\mu_B$ to $3\mu_B$, showing that different multiplicities are really close in energy. However, for the I_h structure, the states with higher spins (multiplicity=22–24)

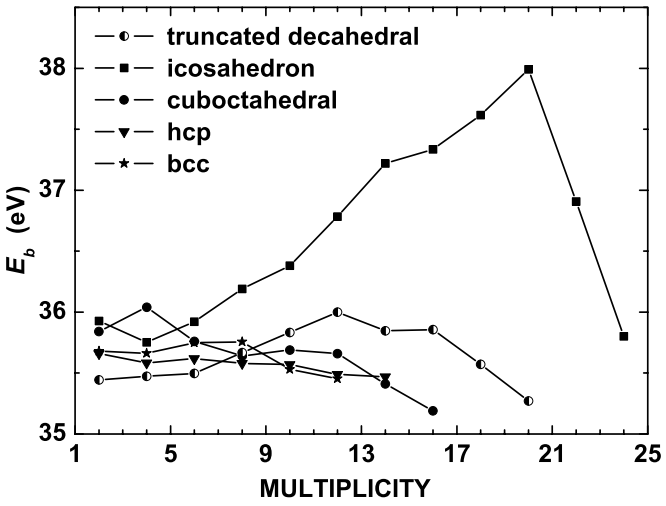

FIG. 10. Variation of E_b as a function of magnetic moments of icosahedron (I_h), truncated decahedral (D_{5h}), bcc (D_{4h}), hcp (D_{3h}), and fcc (O_h) structures for Sc_{13}.

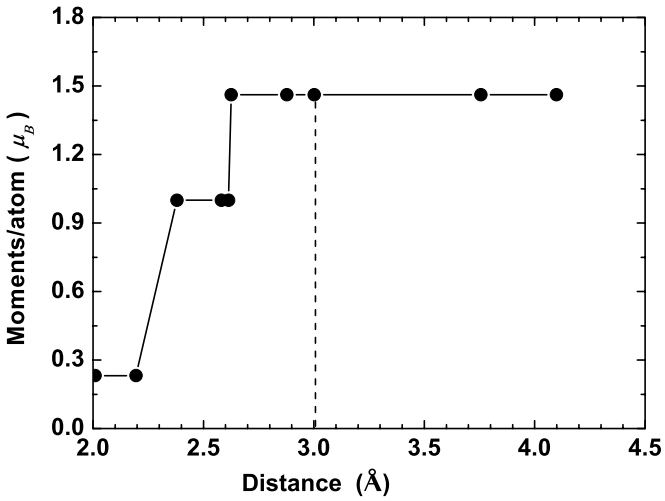

FIG. 11. Variation of magnetic moment vs interatomic distance in icosahedron of Sc_{13} cluster.

are about 1.09–2.19 eV higher than the ground state, while the states with lower spins (multiplicity=2–18) are 0.38–2.07 eV higher in energy than the ground state. Considering such large energy differences, the ground state mixing with the excited states is thus excluded as the possible source of the discrepancy. Based on these analysis, we guess that the experiment value about magnetic moments of Sc_{13} may produced in two isomeric forms at least, in which case the experimentally measured moment is an average value weighted according to the relative abundances of the isomers in the beam quantities that cannot be determined with high precision. We will systemically analyze the difference between theory and experiment in the following paragraph.

In order to test how sensitive the magnetic properties are to the changes in interatomic distances and if these slight changes may be the origin of the discrepancies, we have performed uniform compressions and expansions of the icosahedral Sc_{13} structure. In Fig. 11, we present the results of magnetic moments as a function of r (the distance between the center atom and the vertex atom) for the Sc_{13} cluster. The total moments of the I_h cluster increase from $3\mu_B$ to $13\mu_B$ to $19\mu_B$ with the increase of r. In a wide range of r (2.7 Å$\leqslant r \leqslant$4.5 Å), the total moments remain unaltered. Therefore, we deduce that the magnetic moments of Sc_{13} cluster are not very sensitive to the changes in the interatomic distances around the equilibrium structure, and one speculates there would be small deviations of the magnetic moments using different theoretical methods. In addition, we also notice that a sudden transition from a ferrimagnetic to a ferromagnetic state with a total moment of $19\mu_B$ occurring when the bondlength (between center and vertex atoms) is 2.63 Å. This is about 13% shorter than the equilibrium bonding length of 3.02 Å.

Dunlap[40] observed the dependence of magnetic moment on interatomic distance in Fe clusters. Then the similar phenomena is also found in Rh clusters and explained by Reddy *et al.*,[21] who think that these progressions could be related to the distribution of the levels in the one electron spectrum. We now give the energy spectrum in Fig. 12 and further analyze this aspect with respect to the case of Rh_{13}.[21] In Fig. 12, the numbers represent the electron occupation numbers in the HOMO. The solid lines refer to the occupied states and the dot lines refer to the unoccupied states. For each of the three groups, the lines on the left represent the majority electrons and those on the right represent the minority electrons. Starting from the first group in Fig. 12 (the structure with $3\mu_B$ moments), the HOMO has a threefold degeneracy (T_{1u}) but only one electron. At a distance of 2.38 Å ($13\mu_B$), it is then energetically favorable to transfer five electrons from the minority states to the majority states so that the gain in exchange energy is higher than the kinetic energy needed to occupy the higher-energy states, and the cluster spin states have another set of unoccupied triply degenerate states (T_{1u}) close to HOMO (T_{2u}) which is fully occupied by minority electrons. Further increase in interatomic spacing leads to a transfer of three additional minority electrons to the majority states. Finally, the cluster reaches its equilibrium structure and has the ground state with $19\mu_B$. Thus, the variation in the magnetic moments is intimately linked to the electronic structure.

To better understand the magnetic progress along with the bondlength, we further give the total density of state (TDOS) of I_h Sc_{13} cluster and the local density of state (LDOS) of the center-site Sc atom for majority spin and minority spin electrons in three configurations (in Fig. 13). The DOS was obtained by a Lorentzian extension of the discrete energy levels and summation over them. The broadening width parameter was chosen to be 0.15 eV. The solid lines donate the TDOS for Sc_{13} cluster and the dots donate the LDOS for the central-sited Sc atom. In Fig. 13, the common characteristic feature is the enhancement in the exchange splitting with an increase in bondlength. We also notice that a little upward shift for spin-up band occurs in which the Fermi energy (E_f) locates exactly at or immediately above peaks, while there is a prominent upward shift in spin-down band and the E_f level lies in the digressive minimum of the density of states. The TDOSs of three configurations are similarity in both spin-up

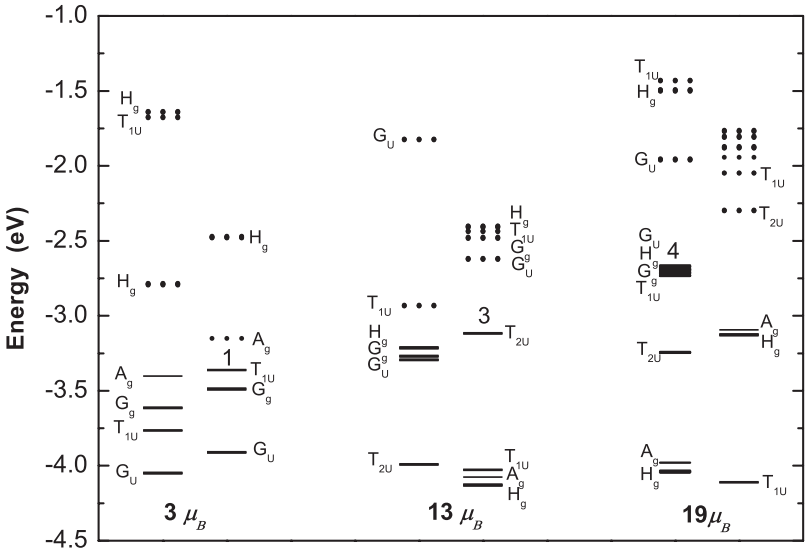

FIG. 12. The energy spectrum of Sc_{13} cluster for the I_h structure with different interatomic distance.

and spin-down bands except the fact that the weight of spin-up peak increases significantly around the E_f. There are two factors, which contribute to the high DOS near the E_f. First, the high I_h symmetry of the cluster results in a large degeneracy for the electronic states, then this large degeneracy produces a high DOS. Second, at a short distance the interactions between the d bands of the surface atoms and d states of the center atom are strong, so that the centroids of their LDOS are energetically well separated and the hybridization will be small. As the distance is increased, the bandwidth decreases due to decreasing overlap. This would also result in a higher DOS peak around the Fermi level. As the exchange splitting increases, the filling of the spin-up band will increase at the cost of the spin-down band, hence the spin moments will increase. The DOS in upper panel (a) has a largest exchange splitting about 0.38 eV, as is consistent with the results of the giant moments.

D. Sc_{13}, Y_{13}, and La_{13} clusters

The particular stability, existence of larger HOMO-LUMO gap and larger magnetic moments suggest that a similar behavior could arises for Y_{13} and La_{13} clusters due to the narrowing bands as Y and La atoms are isoelectronic. In recent theoretical studies,[32,41–44] the results imply that Y_{13} and La_{13} clusters also prefer the icosahedral geometries, having I_h symmetry and D_{2h} symmetry, respectively. After their analysis, they think that the D_{2h} structure of La_{13} as the outcome of distortion from the I_h structure according to the Jahn-Teller theorem.[44] Moreover, the size variations of the average atomic moments of scandium clusters and yttrium clusters in experiment display many of the same features (e.g., local maxima at n=6, 8, 13, and 18).[13] This similarity may imply a common structural motif for two series of Sc and Y clusters other than another series of La clusters (bulk Sc and Y both adopt hcp packing, but bulk La adopts doublet hcp packing). To confirm this viewpoint, we also studied the electronic structures of Y_{13} and La_{13} clusters of icosahedron structure, fcc (O_h) structure and hcp structure. For scandium and yttrium, we considered the all electrons calculation, while for lanthanum, the calculations were performed by considering fully all electrons relativistic (AE relativity).

The ground structures obtained for Sc_{13}, Y_{13}, and La_{13} clusters are icosahedrons with I_h, I_h, and D_{2h} symmetry, respectively. We give the calculated binding energies, HOMO (n), HOMO-LUMO gaps, and magnetic moments in Table I. The HOMO-LUMO gaps in all the three cases are comparable but it is the largest for Sc_{13}. It should be noted that Sc_{13} and Y_{13} clusters have the same larger total magnetic moments of $19\mu_B$ and close-shelled electron structure which means that they would not suffer Jahn-Tell distortion to change their high symmetry structures and moments. The magnetic moments of $1.46\mu_B$/atom in Sc_{13} can compare with localized moments of $1.65\mu_B$ in bulk scandium based on Curie-Weiss analysis of susceptibilities by Spedding and Croat.[45] Icosahedrons with high symmetry and low mean coordination could lead to important changes in the electronic structure with significant consequences for the high magnetic of Sc_{13} and Y_{13} clusters. As might be expected, those atoms with highest coordination in the center have smaller spin densities and the lower-coordinated surface atoms have the highest spin densities. The E_b, DOS and magnetic moments of Y_{13} cluster compare well with previous theory work,[41] and the features in the DOSs of Sc_{13} and Y_{13} are quite similar. As discussed before, the high DOS and large exchange splitting lead to the high magnetic moments. For the La_{13} cluster, the binding energy of I_h structure is 0.21 eV lower than that of the D_{2h} structure, and it is worth noting that $3\mu_B$ magnetic moments of the D_{2h} structure we calculated fit with the experiment[13] better than previous work does.[42–44] The divergence between our calculated values and previous work may be the caused by the different exchange and correlation function used.

In this case, we cannot deal with Sc clusters with orbital magnetic moment and noncollinear configuration. But we can still conclude that the total magnetization of Sc clusters including orbital magnetic moment and noncollinear configuration would represent a considerable improvement with respect to the experiment. Therefore, the differences between theory and experiment may be due to the following one or

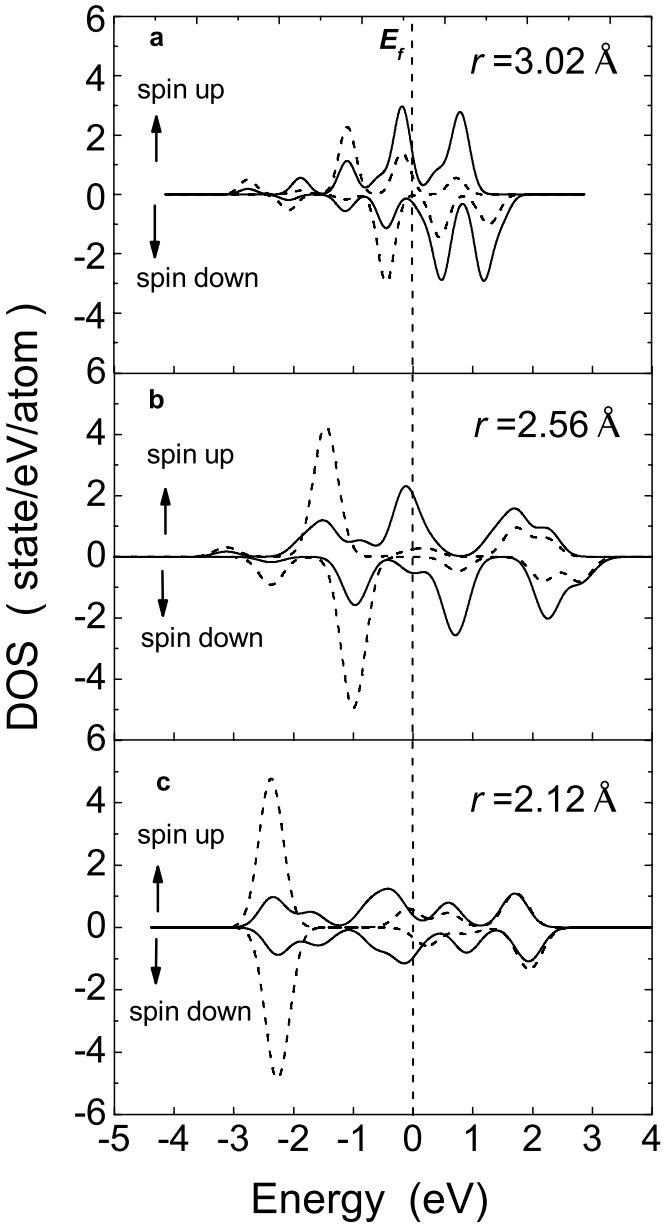

FIG. 13. The DOS of Sc_{13} cluster for the I_h structure with different interatomic distance.

more of several reasons. (1) Various isomers of a given Sc cluster exhibit multitudinal spin multiplicities, and the measured value is an average of multiple lower moment isomers. Since these isomers are energetically nearly degenerate, they could all simultaneously be present in experimental beam. For example, we can see that the second, third, and fourth low-lying isomers $(13b,13c,13d)$ of the Sc_{13} cluster have small moments of $3\mu_B$, which can diminish the difference between experimental and theoretical values. (2) In addition, since the clusters produced in experiment are always at finite temperature T=60 K,[13] it is possible that they are not in their ground states, particularly for those ground states which are energetically close to their excited states. This explanation has recently been proposed by Zhang *et al.*[46] to explain the differences between the predicted magic numbers for neutral C_{60} clusters. (3) For large clusters, the structures we obtained might not be ground state structures or many isomers with little energy difference existing in these clusters. (4) We also note that our investigation is strictly limited to studying the spin contributions to the net cluster moment in that we do not include orbital contributions or more complex (e.g., noncollinear) arrangement of spins. Thus, it could be interesting to have additional experiments, which can eliminate some of the current uncertainties.

IV. CONCLUSION

In summary, motivated by the anomalous magnetism as is observed in condensed phase clusters in experiment, we have determined the geometry structures, binding energies, and electronic and magnetic properties of small Sc_n (n=2–16) clusters with DFT using the GGA exchange-correlation potential method. The main conclusions are as follows. (1) Three lowest energy isomers for each size of Sc_n (n=2–16) clusters are obtained. For the global minimum, we found that the closed compact arrangements dominate for small clusters. In particular, Sc_{13} has a perfect icosahedral structure with the highest stability. (2) The size dependence of binding energies, second difference of energies, ionization potential, electron affinity, and HOMO-LUMO gap are discussed for the Sc clusters. The results indicate that the clusters with $n=4,5,7,10,13$ are more stable than their neighbors. (3) We obtained the general tendency of the magnetic moment as the cluster size approaches n=16 and good quantitative agreement with experiment is found for n=5, 7–12, and 15–16 atoms. The clusters undergo a change from ferromagnetic (FM) ordering for the smallest sizes ($n<7$) to antiferromagnetic (AF) ordering for the intermediate and beyond sizes (n=7–12,15–16). The magnetic behavior of the

TABLE I. The binding energy E_b (eV), nearest neighbor bondlengths R (Å), HOMO-LUMO gap (eV), the atomic moments of the surface atom $M_{\text{surface}}(\mu_B)$ and center atom $M_{\text{center}}(\mu_B)$ for Sc_{13}, Y_{13}, and La_{13} clusters. The HOMO states (symmetry) and the electron occupation numbers n in HOMO. For La_{13} with D_{2h} symmetry, the value R is the average value of $R_{\text{center-vertex}}$ and M_{surface} is the average of the surface atomic magnetic moments.

Cluser	E_b(eV)	R(Å)	HOMO(n)	Gap(eV)	$M_{\text{surface}}(M_{\text{center}})$	Previous work	Experiment (Ref. 13)
$Sc_{13}(I_h)$	37.987	3.002–3.157	$+G_u(4)$	0.472	1.563(0.247)		$6.0\pm0.2\mu_B$
$Y_{13}(I_h)$	40.017	3.313–3.484	$+T_{1u}(3)$	0.245	1.576(0.083)	$13\mu_B$ (Ref. 32), $19\mu_B$ (Ref. 41)	$8.8\pm0.1\mu_B$
$La_{13}(I_h)$	45.087	3.451–3.629	$+H_g(5)$	0.187	1.124(−0.494)	$3\mu_B$ (Refs. 42–44)	$2.1\mu_B$
$La_{13}(D_{2h})$	45.301	3.485	$+A_g(1)$	0.186	0.256(−0.068)	$1\mu_B$ (Refs. 42–44)	

Sc_{13} cluster is extensive investigated and the variation in the magnetic moments is intimately linked to the electronic structure. (4) We also analyzed the discrepancy of the magnetic moments between experiment and calculation. We hope the results will stimulate experiments further to study small scandium clusters.

ACKNOWLEDGMENTS

This work was supported by the National Natural Science Foundation of China (Project No. 10575083) and the Chongqing's Natural Science Foundation of China (Contract No. 8111).

*Email address: chenh@swu.edu.cn

[1] M. B. Knickelbein, Phys. Rev. Lett. **86**, 5255 (2001).
[2] M. B. Knickelbein, Phys. Rev. B **70**, 014424 (2004).
[3] A. J. Cox, J. G. Louderback, and L. A. Bloomfield, Phys. Rev. Lett. **71**, 923 (1993).
[4] L. A. Bloomfield, J. Deng, H. Zhang, and J. W. Emmert, in *Proceedings of the International Symposium on Cluster and Nanostructure Interface*, edited by P. Jena, S. N. Khanna, and B. K. Rao (World Publishers, Singapore, 2000), p. 131.
[5] P. C. Hohenberg and W. Kohn, Phys. Rev. **136**, B864 (1964).
[6] W. Kohn and L. J. Sham, Phys. Rev. **140**, A1133 (1965).
[7] E. O. Berlanga-Ramrez, F. Aguilera-Granja, A. Daz-Ortiz, J. L. Rodriguez-Lopez, and A. Vega, Phys. Lett. A **318**, 473 (2003).
[8] K. Lee and J. Callaway, Phys. Rev. B **49**, 13906 (1994).
[9] D. C. Douglass, J. P. Bucher, and L. A. Bloomfield, Phys. Rev. B **45**, 6341 (1992).
[10] J. F. Janak, Phys. Rev. B **16**, 255 (1977).
[11] L. B. Knight, R. J. Van Zee, and W. Weltner, Chem. Phys. Lett. **94**, 296 (1983).
[12] M. Moskovits, D. P. Dilella, and W. Limm, J. Chem. Phys. **80**, 626 (1984).
[13] M. B. Knickelbein, Phys. Rev. B **71**, 184442 (2005).
[14] S. Yanasigava, T. Tsuneda, and K. Hirao, J. Chem. Phys. **112**, 545 (2000).
[15] G. L. Gutsev, P. Jena, B. K. Rao, and S. N. Khanna, J. Chem. Phys. **114**, 10738 (2001).
[16] V. Kumar and Y. Kawazoe, Phys. Rev. B **65**, 125403 (2002).
[17] DMOL, v960, Biosym Technologies, San Diego, CA, 1996.
[18] J. P. Perdew and Y. Wang, Phys. Rev. B **45**, 13244 (1992).
[19] A. D. Becke, Phys. Rev. A **38**, 3098 (1988).
[20] V. Kumar and Y. Kawazoe, Phys. Rev. B **66**, 144413 (2002).
[21] B. V. Reddy, S. K. Nayak, S. N. Khanna, B. K. Rao, and P. Jena, Phys. Rev. B **59**, 5214 (1999).
[22] Q. Wang, Q. Sun, B. K. Rao, P. Jena, and Y. Kawazoe, J. Chem. Phys. **119**, 7124 (2003).
[23] O. Dieguez, M. M. G. Alemany, C. Rey, P. Ordejon, and L. J. Gallego, Phys. Rev. B **63**, 205407 (2001).
[24] J. L. Wang, G. H. Wang, and J. J. Zhao, Phys. Rev. B **66**, 035418 (2002).
[25] F. Aguilera-Granja, J. L. Rodriguez-Lopez, K. Michaelian, E. O. Berlanga-Ramirez, and A. Vega, Phys. Rev. B **66**, 224410 (2002).
[26] M. Castro, C. Jamorsky, and D. R. Salahub, Chem. Phys. Lett. **271**, 133 (1997).
[27] M. Castro, Int. J. Quantum Chem. **64**, 223 (1997).
[28] M. Castro and D. R. Salahub, Phys. Rev. B **49**, 11842 (1994).
[29] M. Matsumoto, J. B. Staunton, and P. Strange, J. Phys.: Condens. Matter **3**, 1453 (1991).
[30] V. Kumar, K. Esfariani, and Y. Kawazoe, in *Clusters and Nanomaterials*, edited by Y. Kawazoe, T. Kondow, and K. Ohno, Springer Series in Cluster Physics (Springer-Verlag, Heidelberg, 2002), p. 9.
[31] V. Kumar and Y. Kawazoe, Phys. Rev. B **63**, 075410 (2001).
[32] Kraiming Deng, Jinlong Yang, Chuanyun Xiao, and Kelin Wang, Phys. Rev. B **54**, 11907 (1996).
[33] F. S. Ham, J. Lumin. **85**, 193 (2000).
[34] C. Kohl and G. F. Bertsch, Phys. Rev. B **60**, 4205 (1999).
[35] H. Cheng and L. S. Wang, Phys. Rev. Lett. **77**, 51 (1996).
[36] R. C. Longo, E. G. Noya, and L. J. Gallego, J. Chem. Phys. **122**, 226102 (2005).
[37] T. Morisato, S. N. Khanna, and Y. Kawazoe, Phys. Rev. B **72**, 014435 (2005).
[38] R. A. Guirado-Lopez, J. Dorantes-Davila, and G. M. Pastor, Phys. Rev. Lett. **90**, 226402 (2003).
[39] X. G. Wan, L. Zhou, J. M. Dong, T. K. Lee, and D. S. Wang, Phys. Rev. B **69**, 174414 (2004).
[40] B. I. Dunlap, Phys. Rev. A **41**, 5691 (1990).
[41] C. G. Ding, J. L. Yang, Q. X. Li, K. L. Wang, and F. Toigo, Phys. Lett. A **256**, 417 (1999).
[42] D. B. Zhang and J. Chen, J. Chem. Phys. **123**, 049903 (2005).
[43] D. B. Zhang and J. Chen, J. Chem. Phys. **120**, 5104 (2004).
[44] D. B. Zhang and J. Chen, J. Chem. Phys. **120**, 5081 (2004).
[45] F. H. Spedding and J. J. Croat, J. Chem. Phys. **58**, 5514 (1973).
[46] W. Zhang, L. Liu, J. Zhuang, and Y. Li, Phys. Rev. B **62**, 8276 (2000).